

See discussions, stats, and author profiles for this publication at: <https://www.researchgate.net/publication/260306184>

Ionic Grubbs–Hoveyda Complexes for Biphasic Ring–Opening Metathesis Polymerization in Ionic Liquids: Access to Low Metal Content Polymers

ARTICLE *in* CHEMCATCHEM · JANUARY 2014

Impact Factor: 4.56 · DOI: 10.1002/cctc.201300751

CITATIONS

7

READS

50

4 AUTHORS, INCLUDING:



Camila Ferraz

University of São Paulo

7 PUBLICATIONS 32 CITATIONS

SEE PROFILE



Wolfgang Frey

Universität Stuttgart

334 PUBLICATIONS 3,712 CITATIONS

SEE PROFILE



Michael R Buchmeiser

Universität Stuttgart

331 PUBLICATIONS 7,628 CITATIONS

SEE PROFILE

Ionic Grubbs–Hoveyda Complexes for Biphasic Ring-Opening Metathesis Polymerization in Ionic Liquids: Access to Low Metal Content Polymers

Camila P. Ferraz,^[a, b] Benjamin Autenrieth,^[a] Wolfgang Frey,^[c] and Michael R. Buchmeiser^{*,[a, d]}

A novel ionic metathesis catalyst, $[\text{Ru}(\text{1-CH}_3\text{-4-CO}_2\text{Py}^+)_2(\text{IMesH}_2)(=\text{CH-2-(2-PrO)-5-NO}_2\text{C}_6\text{H}_3)][\text{OTf}^-]_2$ (**3b**; IMesH₂ = 1,3-dimesitylimidazolin-2-ylidene, Py = pyridine), has been prepared. **3b** and the Grubbs–Hoveyda catalysts $[\text{Ru}(\text{1-CH}_3\text{-4-CO}_2\text{Py}^+)_2(\text{IMesH}_2)(=\text{CH-2-(2-PrO)C}_6\text{H}_4)][\text{OTf}^-]_2$ (**3a**) and $[\text{RuCl}(\text{1-CH}_3\text{-4-CO}_2\text{Py}^+)(\text{IMesH}_2)(=\text{CH-2-(2-PrO)C}_6\text{H}_4)][\text{OTf}^-]$ (**5a**) were used for ring-opening metathesis polymerization (ROMP) reactions under both homogeneous and biphasic liquid–liquid conditions by using the ionic liquid 1-butyl-2,3-dimethylimidazolium tetrafluoroborate ($[\text{BDMIM}^+][\text{BF}_4^-]$) and toluene. All catalysts

were active in the ROMP of norborn-2-ene-based monomers, with *cis*-cyclooctene and dicyclopentadiene providing good yields under homogeneous conditions and complex **5a** the most active catalyst. With all catalysts, the use of a chain transfer agent (CTA) allowed for the synthesis of polymers with low metal contents between 10 and 80 ppm, corresponding to a ruthenium removal of 98–99.8% without any additional purification step. In addition, the use of a CTA allowed for recycling experiments under biphasic conditions, in which **3a** and **5a** were particularly active for several cycles.

Introduction

Olefin metathesis is nowadays considered one of the most important reactions for the formation of carbon–carbon bonds with a wide range of applications in organic chemistry, polymer chemistry, and materials science.^[1–6] However, especially when it comes to the production of fine chemicals, substantial challenges remain in terms of catalyst separation and recycling.^[7–10] Many immobilization strategies for metathesis catalysts have been reported,^[11–17] most of which entail the anchoring of the metathesis catalysts onto various organic and inorganic supports.^[11–17] In addition, non-covalent approaches have been developed for the immobilization of metathesis catalysts.^[18–20] By using supported ionic-liquid phase (SILP) technology for metathesis reactions, continuous metathesis reactions have been realized.^[21] For this purpose, cationic complexes

such as $[\text{Ru}(\text{DMF})_3(\text{IMesH}_2)(=\text{CH-2-(2-PrO)C}_6\text{H}_4)^{2+}][\text{BF}_4^-]_2$ (DMF = *N,N*-dimethylformamide) have been created. Ring-closing metathesis (RCM) and cross-metathesis (CM) reactions have been performed under homogeneous and continuous biphasic conditions with low ruthenium leaching and high turnover numbers.^[21,22]

Surprisingly, there are only a few reports on biphasic polymerization reactions.^[20,23–26] This owes mostly to poor separation opportunities if neutral olefin metathesis catalysts are used. In contrast, an ionic initiator would allow for ROMP reactions under biphasic liquid–liquid conditions.^[27] Such an initiator could be dissolved in a polar liquid, for example, an ionic liquid (IL) phase,^[28] whereas both the monomers and polymers would dissolve in a second nonpolar, liquid phase. For a good separation of the ionic catalyst and the final polymers, however, the use of a chain transfer agent (CTA) to provoke the release of the catalyst from the growing polymer chain is mandatory. After successful cleavage, the catalyst would remain in the polar liquid phase and the corresponding polymer with a low metal content would dissolve in the nonpolar phase. Depending on the stability of the catalyst, such an approach would also allow for its multiple recycling.


Herein, we report the synthesis of a new dicationic alkylidene complex $[\text{Ru}(\text{1-CH}_3\text{-4-CO}_2\text{Py}^+)_2(\text{IMesH}_2)(=\text{CH-2-(2-PrO)-5-NO}_2\text{C}_6\text{H}_3)][\text{OTf}^-]_2$ (**3b**; Py = pyridine) for ROMP reactions under homogeneous and biphasic liquid–liquid conditions by using the IL 1-butyl-2,3-dimethylimidazolium tetrafluoroborate ($[\text{BDMIM}^+][\text{BF}_4^-]$) and toluene. The aim was to study initiator behavior under biphasic conditions and investigate the possibility of catalyst recycling. The catalyst is also compared to the di- and monocationic complexes $[\text{Ru}(\text{1-CH}_3\text{-4-CO}_2\text{Py}^+)_2(\text{IMesH}_2)(=\text{CH-2-(2-PrO)C}_6\text{H}_4)][\text{OTf}^-]_2$ (**3a**) and $[\text{RuCl}(\text{1-CH}_3\text{-4-}$

[a] C. P. Ferraz, B. Autenrieth, Prof. M. R. Buchmeiser
Lehrstuhl für Makromolekulare Stoffe und Faserchemie
Institut für Polymerchemie
Universität Stuttgart
Pfaffenwaldring 55, 70569 Stuttgart (Germany)
Fax: (+49) 711-685-64050
E-mail: michael.buchmeiser@ipoc.uni-stuttgart.de

[b] C. P. Ferraz
Instituto de Química de São Carlos
Universidade de São Paulo
CP 780, 13560-970, São Carlos - SP (Brazil)

[c] Dr. W. Frey
Institut für Organische Chemie
Universität Stuttgart
Pfaffenwaldring 55, 70569 Stuttgart (Germany)

[d] Prof. M. R. Buchmeiser
Institut für Textilchemie und Chemiefaser (ITCF) Denkendorf
Körschtalstr. 26, 73770 Denkendorf (Germany)

 Supporting information for this article is available on the WWW under <http://dx.doi.org/10.1002/cctc.201300751>.

$\text{CO}_2\text{Py}^+(\text{IMesH}_2)(=\text{CH}-2\text{-}\{2\text{-PrO}\}\text{C}_6\text{H}_4)[\text{OTf}^-]$ (**5a**) to evaluate how the nitro group in the alkylidene moiety affects initiation efficiency.

Results and Discussion

Syntheses and structures of ruthenium complexes **2b**, **4b**, and **3b**

The precursor $[\text{RuCl}_2(\text{IMesH}_2)(=\text{CH}-2\text{-}\{2\text{-PrO}\}-5\text{-NO}_2\text{C}_6\text{H}_3)]$ (**1b**) shows, besides excellent air-stability and partial recyclability,^[29–31] high activity in various types of metathesis reactions (RCM, CM, enyne metathesis). Complexes **2b** and **4b** are synthesized by adding one or two equivalents of $\text{CF}_3\text{SO}_3\text{Ag}$ to **1b**, analogous to the syntheses of complexes **2a** and **4a** (Scheme 1).^[32]

Interestingly, the presence of the nitro group in the alkylidene moiety results in slower substitution reactions. Thus, formation of **2b** takes four times longer than that of **2a**; formation of **4b** takes two times longer than for **4a**. In CH_2Cl_2 , the formation of AgCl is fast, resulting in the formation of a cationic intermediate. THF, as a weakly coordinating solvent, seems to stabilize the intermediate.

Complex **2b** crystallizes in the monoclinic space group $P2_1/n$, $a=1176.29(8)$ pm, $b=2023.72(14)$ pm, $c=1617.41(9)$ pm, $\beta=93.837^\circ$, $Z=4$ (Figure 1 and Tables S1–S6, Supporting Information). Complex **4b** crystallizes in the monoclinic space group $P2_1/c$, $a=1019.08(6)$ pm, $b=1908.96(11)$ pm, $c=1793.84(10)$ pm, $\beta=92.332^\circ$, $Z=4$ (Figure 2 and Tables S7–S11, Supporting Information). Selected bond lengths and angles are given in Table 1. Both complexes are d^6 low-spin complexes with a distorted trigonal bipyramidal ligand sphere around the ruthenium with the NHC and the 2-PrO ligands in apical positions. The ruthenium–alkylidene bond is slightly shorter in **2b** than in **4b**, indicating stronger polarization. Similarly, the ruthenium–oxygen bond in the 2-PrO-benzylidene ligand is shorter in **2b** than in **4b**, indicating a slightly stronger ruthenium–oxygen bond. Both findings are in accordance with the highly electron withdrawing character of the triflate group.

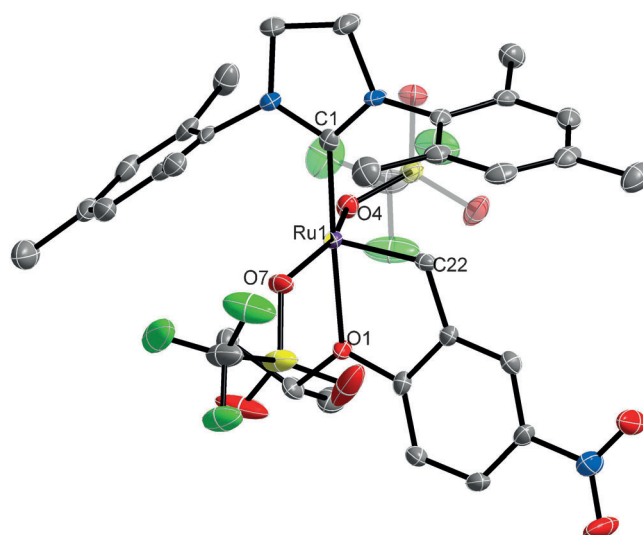


Figure 1. X-ray structure of **2b**.

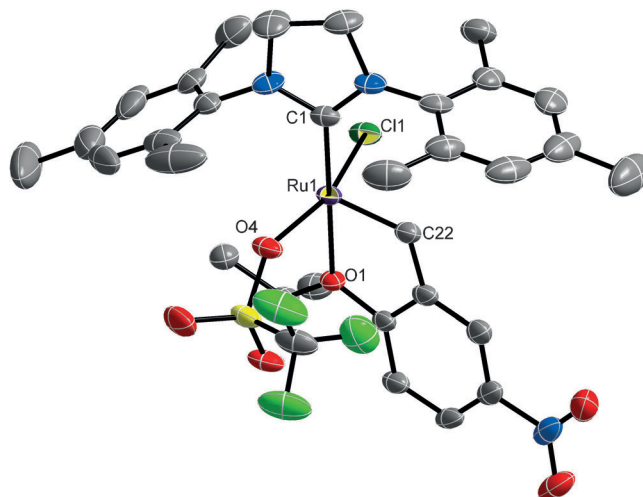
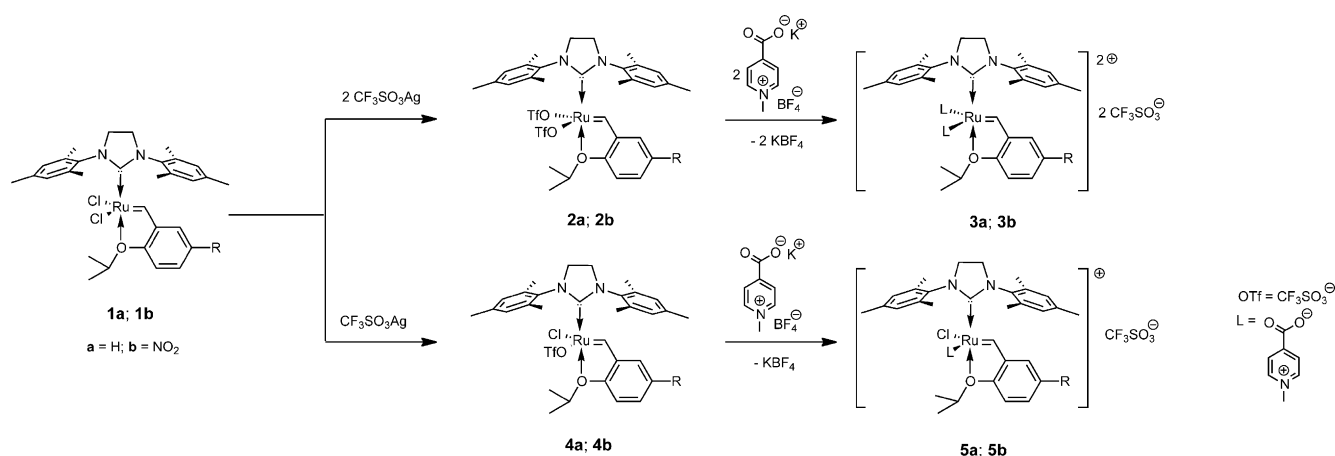


Figure 2. X-ray structure of **4b**.



Scheme 1. Syntheses of catalysts **2a**, **2b**, **3a**, **3b**, **4a**, **4b**, **5a**, and **5b**.

Table 1. Selected bond lengths and angles of **2b** and **4b**.

Bond	2b	4b	4a ^[32]
<i>Bond length [pm]</i>			
Ru1–C22	182.6(3)	183.0(3)	182.0(3)
Ru1–C1	199.7(3)	200.0(3)	198.4(4)
Ru1–O4	206.3(2)	210.70(18)	209.86(19)
Ru1–O7	207.6(2)	–	–
Ru1–O1	223.1(2)	223.37(16)	224.99(17)
Ru1–Cl1	–	231.35(7)	231.82(7)
<i>Bond angle [°]</i>			
C22–Ru1–C1	99.37(14)	102.02(12)	102.34(11)
C22–Ru1–O4	100.14(12)	98.58(10)	98.87(10)
C22–Ru1–O7	99.29(12)	–	–
C22–Ru1–O1	79.15(11)	79.65(10)	79.31(10)
C22–Ru1–Cl1	–	98.62(9)	97.21(9)
C1–Ru1–O4	93.27(11)	90.76(9)	93.50(9)
C1–Ru1–O7	94.21(11)	–	–
C1–Ru1–O1	176.93(11)	177.13(9)	178.17(8)
C1–Ru1–Cl1	–	92.04(8)	93.12(7)
O4–Ru1–O7	157.73(9)	–	–
O4–Ru1–O1	84.38(9)	91.30(6)	85.43(7)
O4–Ru1–Cl1	–	161.59(6)	160.87(6)
O7–Ru1–O1	88.69(8)	–	–

Generally, the distances found in **4b** are comparable to those reported for **4a**, which does not contain a nitro group in the benzylidene ligand.

The dicationic complex **3b** was prepared in a similar manner to complex **3a** by adding 2.3 equivalents of the ionic ligand $[(1\text{-CH}_3)(4\text{-CO}_2\text{K})\text{Py}]^+[\text{BF}_4]^-$ to complex **2b** (Scheme 1). As for complex **3a**, both triflate ligands were replaced by two mole-

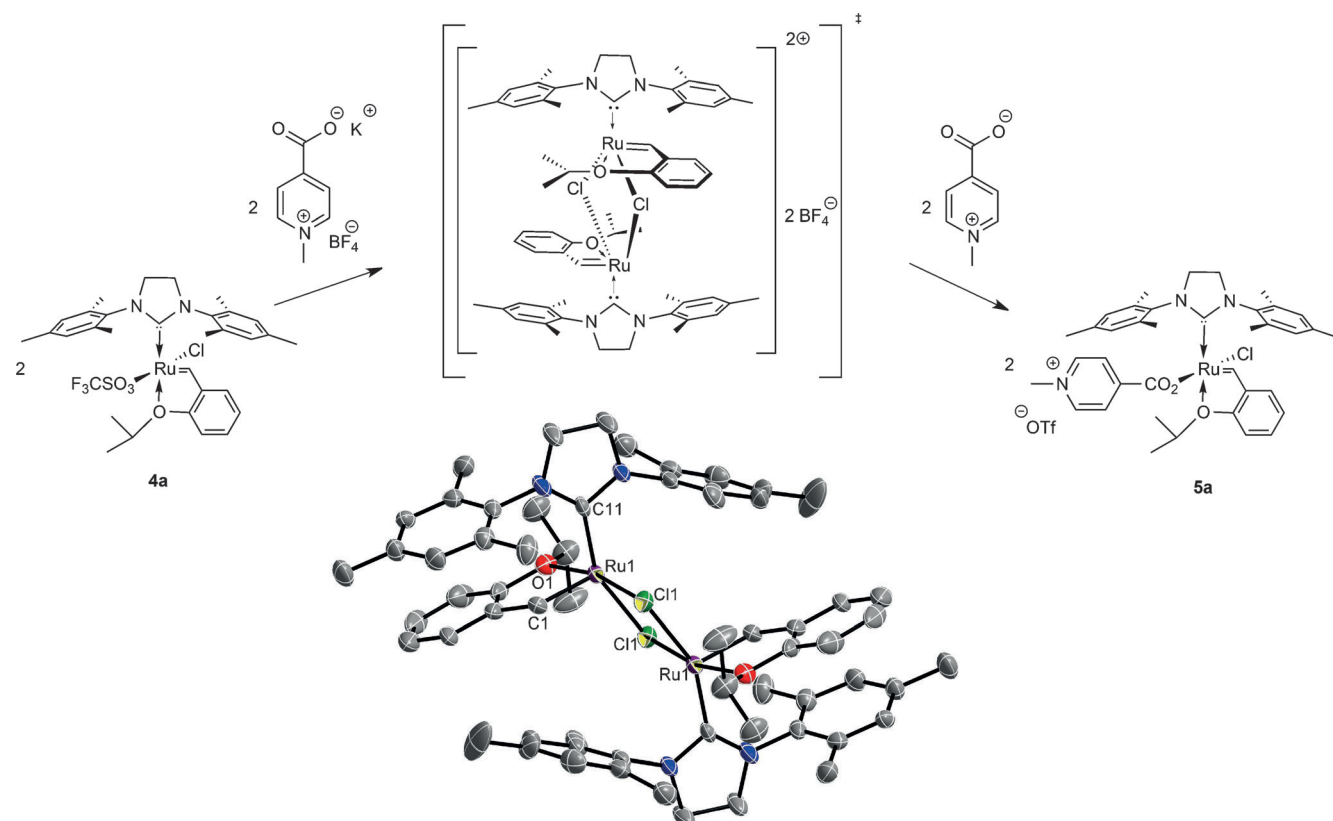
cules of the ionic ligand and ended up as the counter ions. In contrast to monoionic **5a**,^[22] the corresponding monoionic complex **5b** could not be isolated. During the preparation of complex **5b**, fast disproportionation to the corresponding bis-chloride and bis-carboxylate complexes **1b** and **3b** was observed (Figure S6, Supporting Information). The same reaction was described for **3a**, however, it took much longer.^[22]

During the synthesis of **5a**, a dichlorido-bridged dimer intermediate was isolated (Scheme 2). Selected bond lengths and angles are given in Tables S12–S16 in the Supporting Information. This clearly indicated that substitution of the triflate was fast and the resulting intermediate was stabilized through dimerization.

The ¹H NMR spectrum of **3b** shows a downfield shifted alkylidene signal at $\delta = 18.18$ ppm, indicative of a strong polarization of the ruthenium–carbon bond similar to **3a** (Table 2). Generally, the nitro group in the alkylidene moiety gives rise only to subtle differences in the chemical shifts compared to **3a**. If the chlorido ligands are replaced by pseudo-halides, the more electron-withdrawing triflate ligand induces a more pronounced downfield shift of the alkylidene signal than the $[(1\text{-CH}_3)(4\text{-CO}_2)\text{Py}]^+$ ligand (Table 2).

ROMP reactions under homogeneous conditions

At 40 °C, catalyst **5a** was active in the ROMP of norborn-2-ene (NBE), *cis*-cyclooctene (COE), dicyclopentadiene (DCPD), 5-(4-butylphenyl)norborn-2-ene (NBE-Ph) and 5-(decyloxymethyl)-norborn-2-ene (NBE-OC₁₀H₂₁) (Table 3, entries 11–14). Yields



Scheme 2. Crystal structure of the isolated dimer intermediate from the synthesis of **5a**.

Table 2. ^1H NMR alkylidene shifts of complexes **1a**, **1b**, **2a**, **2b**, **3a**, and **3b**.

Ligand	δ [ppm] ^[a]	
Cl^-	16.56 (1a) ^[33]	16.47 (1b) ^[29–31]
CF_3CO_2^-	17.38 ^[34]	17.28 ^[34]
CF_3SO_3^-	18.49 (2a) ^[32]	18.68 ^[b] (2b)
$[(1-\text{CH}_3)(4-\text{CO}_2)\text{Py}^+]$	18.23 ^[b] (3a) ^[22]	18.18 ^[b] (3b)

[a] In CDCl_3 , [b] In CD_2Cl_2 .

were in the range of 80–100%, polydispersity indices (PDIs) were in the range of 1.4–2.4. Catalyst **3b** also displayed good activity in NBE polymerization, reaching 90% yield within 2 h using a catalyst loading of 0.1 mol% (Table 3, entry 1). Catalyst **3a** was highly active in the polymerization of NBE but gave poor results with the other monomers. As observed with many other Grubbs–Hoveyda-type catalysts,^[35,36] the dissociation of the 2-propoxy group was slow compared to propagation. Thus, a k_p/k_i (k_p = rate constant of polymerization, k_i = rate constant of initiation)^[37] value of >10 was recorded for **3b**. In some cases, the experimentally determined number-average molar weight (M_n) values of the poly(NBE) materials (Table 3, entries 1 and 2) were higher than the theoretical ones, indicating incomplete initiation. Except for NBE-OC₁₀H₂₁ (Table 3, entry 8), the *cis/trans* content of the NBE-based monomers (i.e., NBE and NBE-Ph) was approximately 50:50. These results showed that the ruthenium alkylidenes bearing cationic ligands presented here did not have any advantage over their neutral analogues if used in homogeneous ROMP, with one important exception: unlike other ruthenium- (and molybdenum-) based catalysts, **3b** polymerized DCPD to yield linear, soluble poly(DCPD) without any cross-linking (Table 3, entries 6 and 7).

ROMP of NBE under biphasic conditions

Next, ROMP reactions were performed under biphasic conditions with $[\text{BDMIM}^+][\text{BF}_4^-]$ as the IL phase and toluene as the second liquid phase. The IL chosen had a non-coordinating anion, preventing ligand scrambling,^[21,22,28] and a very poor miscibility with common nonpolar organic solvents, such as toluene, diethyl ether, heptane, or hexane.

As in previous reports on the ROMP in ILs,^[21,22,27,28] a catalyst loading of 0.5 mol% was chosen. Both the monomer concentration and reaction times were the same as in the ROMP under homogeneous conditions. A CTA was required to release the complex from the polymer chain, preventing ruthenium leaching and allowing for catalyst recycling. For these purposes, $(1-\text{C}_2\text{H}_5)(2-[2-\text{PrO}]) (5-\text{NO}_2)\text{C}_6\text{H}_3$ was used for **3b** and $(1-\text{C}_2\text{H}_5)(2-[2-\text{PrO}])\text{C}_6\text{H}_4$ for **3a** and **5a**. The functional styrenes could be added at the end or at the beginning of the polymerization reaction to control both initiation and propagation, resulting in lower

PDIs, as previously reported.^[38,39] If the CTA was added at the beginning of the reaction (Table 4, entry 5, $\text{CTA}_{\text{initial}}/\text{cat.}$ ratio = 10), the lowest molecular weights and the highest PDIs were observed. If the CTA was added at the end of the reaction (Table 4, entries 1–4), the procedure described in the following was performed.

For the ROMP of NBE under biphasic conditions, the catalyst and IL were mixed and heated to 40 °C, upon which the IL melted to form a red solution. Then, the NBE solution in toluene was added by using a syringe. Initially, the dicationic catalyst was insoluble in the toluene phase. Consequently, two phases were observed, one containing the IL and the catalyst (lower) and the other containing toluene and NBE (upper) (Scheme 3, I). During the reaction, the two phases turned into one and viscosity increased over time (Scheme 3, II). Clearly, the growing poly(NBE) chain with the dicationic complex at the end acted as a surfactant, inducing miscibility between the IL and toluene. After two hours, the CTA solution ($\text{CTA}_{\text{final}}$) was added and the two phases reformed immediately, suggesting that the catalyst had been removed from the polymer backbone (Scheme 3, III). The toluene phase was collected and the remaining IL solution was washed with toluene. The washing

Table 3. ROMP reactions under homogeneous conditions with **3b**, **3a**, and **5a**.^[a]

Entry	Cat.	Monomer	Cat. [mol %]	t [h]	Yield [%] ^[d]	M_n (theor.) [g mol ⁻¹]	M_n (exp.) [g mol ⁻¹]	PDI	<i>cis/trans</i>
1	3b	NBE	0.1	2	90	94 000	197 000	4.5	49:51
2			0.5	2 ^[c]	63	19 000	12 000	3.7	51:49
3			0.02	1	3	471 000	39 000	4.1	53:47
4		COE	0.1	2	70	110 000	270 000	1.5	38:62
5			0.5	2 ^[c]	47	22 000	150 000	1.8	37:63
6		DCPD	0.2	2	4	66 000	— ^[e]	—	—
7			0.5	2 ^[c]	4	26 000	61 000	1.8	45:55
8		NBE-OC ₁₀ H ₂₁	0.5	2	49	50 000	105 000	2.3	63:37
9	3a	NBE	0.5	2	100	19 000	16 000	4.1	44:56
10		NBE-OC ₁₀ H ₂₁	0.5	2	10	50 000	87 000	2.2	46:54
11		COE	0.5	2	10	22 000	104 000	1.4	40:60
12	5a	NBE	0.5	2	100	19 000	26 000	2.4	53:47
13		COE	0.5	2	99	22 000	111 000	1.4	23:77
14		NBE-Ph ^[b]	0.5	2	100	45 000	—	—	—
15		NBE-OC ₁₀ H ₂₁	0.5	2	80	50 000	98 000	2.1	50:50

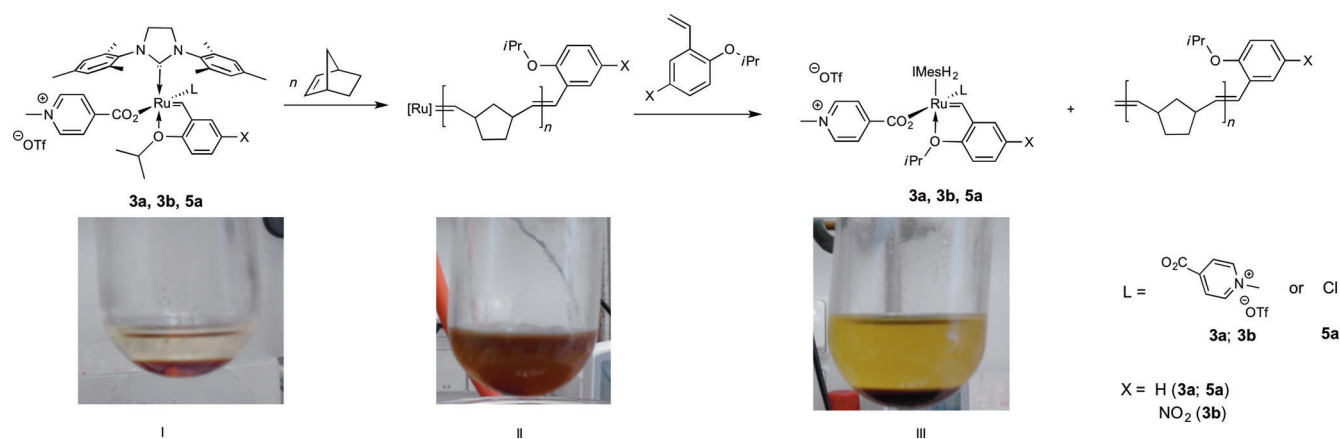
[a] Conditions: $T = 40^\circ\text{C}$, 2 mL CH_2Cl_2 , [b] RT, [c] 0.4 mL CH_2Cl_2 , $[\text{NBE}] = 0.425 \text{ mol L}^{-1}$.

[d] Isolated polymer after precipitation. [e] — = insoluble.

Table 4. ROMP of NBE under biphasic conditions with **3b**.^[a]

Entry	Molar ratio $\text{CTA}_{\text{initial}}/\text{cat.}$	$\text{CTA}_{\text{final}}/\text{cat.}$	t_{CTA} [h] ^[b]	Yield [%]	M_n (exp.) [g mol ⁻¹]	PDI	<i>cis/trans</i>	Ru contamination [ppm]
1 ^[c]	0	5	4	88	72 000	1.9	51:49	84
2 ^[d]	0	5	4	82	24 000	3.8	51:49	83
3	0	100	4	86	7000	1.3	52:48	76
4	0	100	1	86	8800	1.2	50:50	75
5	10	0	0	76	5600	4.0	51:49	72

[a] Conditions: $T = 40^\circ\text{C}$, $t = 2 \text{ h}$, catalyst/monomer molar ratio = 1:200, [catalyst] = 4 mg_{catalyst} per 400 mg_{IL} (8.52 $\mu\text{mol}_{\text{catalyst}} \text{ g}_{\text{IL}}^{-1}$), 1.6 mL toluene, $[\text{NBE}] = 0.425 \text{ mol L}^{-1}$, M_n (theor.) = 19 000 g mol⁻¹. [b] Reaction time with CTA. [c] 3.2 mL toluene, $[\text{NBE}] = 0.212 \text{ mol L}^{-1}$. [d] $t = 1 \text{ h}$, [catalyst] = 4 mg_{catalyst} per 800 mg_{IL} (4.26 $\mu\text{mol}_{\text{catalyst}} \text{ g}_{\text{IL}}^{-1}$).



Scheme 3. ROMP of NBE under biphasic conditions by using **3b**: I) Beginning of the reaction with the IL phase at the bottom and the toluene phase at the top. II) After 1 h reaction, formation of one phase. III) After reaction with the CTA, reformation of the two phases.

procedure was repeated until the toluene phase was colorless and no polymer precipitated upon addition of the toluene phase to methanol. This switching of the ionic catalyst and the initiation behavior were also investigated by ^1H NMR. Quantitative initiation as well as reformation of the starting complex upon treatment with CTA was observed in the polymerization of NBE (Figure S7, Supporting Information).

With **3b**, the experimentally determined M_n values for poly-(NBE) were in the range of 6700–72 000 g mol⁻¹, depending on the monomer/CTA molar ratio. Low PDI values (1.2–1.4) were obtained with both 5 and 100 equivalents of CTA (Table 4, entries 1, 3, and 4) but the use of 100 equivalents of CTA afforded the lowest PDI value of 1.2 (Table 4, entry 4). If the CTA was added at the beginning of the reaction, higher PDIs and a lower yield of polymer were obtained (Table 4, entry 6). In all cases, the amount of CTA used (5 or 100 equiv.) was sufficient to cleave the catalyst from the polymer chain, as shown by the low ruthenium contamination of the different poly(NBE) materials prepared (Table 4). Notably, the ruthenium content of poly(NBE) was ≤ 84 ppm without any additional purification, for example, by precipitation. In view of the molar initiator/monomer ratio used here, this corresponded to a ruthenium removal of 98–99%. In terms of phase separation, 100 equivalents of CTA allowed for a much faster phase separation and the two phases were more defined compared to experiments carried out with 5 equivalents. Notably, excess CTA was fully recovered.

Adding 100 equivalents of CTA at the end of the polymerization reaction, both catalysts **3a** and **5a** allowed for the synthesis of poly(NBE), poly(COE) and poly(NBE-OC₁₀H₂₁) under biphasic conditions. For both catalysts, high molecular weight polymers with PDIs in the range of 1.8–2.4 (Table 5) were obtained. Interestingly, the *cis/trans* ratios differed quite significantly from those obtained in CH₂Cl₂, suggesting a different conformation of the propagating alkylidene. Ruthenium contaminations of the polymers were in the range of 30–86 ppm, which translated into a ruthenium removal of 98–99.4% without an additional purification step.

Table 5. ROMP reactions under biphasic conditions with **3b**, **3a**, and **5a**.^[a]

Entry	Cat.	Monomer	Yield [%]	M_n (exp.) [g mol ⁻¹]	PDI	<i>cis/trans</i>	Ru contamination [ppm]
1	3b	NBEOC ₁₀ H ₂₁	76	4000	1.2	68:32	47
2	3a	NBE	97	131 000	2.3	61:39	53
3		COE	12	–	–	27:73	30
4		NBEOC ₁₀ H ₂₁	65	21 000	2.4	62:38	57
5	5a	NBE	97	89 000	2.1	59:41	86
6		COE	95	78 000	1.8	21:79	33
7		NBEOC ₁₀ H ₂₁	82	94 000	2.3	54:46	85

[a] Conditions: $T=40^{\circ}\text{C}$, $t=2\text{ h}$, catalyst/monomer molar ratio = 1:200; [catalyst] = 4 mg_{catalyst} per 400 mg_{NL} (8.52 μmol_{catalyst} g_{NL}⁻¹), 1.6 mL toluene, [monomer] = 0.425 mol L⁻¹, CTA (100 equiv) added at the end of the reaction, M_n (theor.): poly(NBE) = 18 800 g mol⁻¹, poly(COE) = 22 000 g mol⁻¹, poly(NBE-*O*-C₁₀H₂₁) = 50 000 g mol⁻¹.

Catalyst recycling

Catalyst recycling was tested for the ROMP of NBE by using **3b**, **3a**, and **5a** (Table 6). The CTA was added after 2 h, allowing reaction for an additional 1 h. After removal of the polymer containing phase, the IL phase was extracted with toluene, then fresh NBE was added for the next run. This recycling process is illustrated in Scheme 4.

For **3b** bearing a nitro-substituted benzylidene ligand, only 3 cycles were possible, with a significant decrease in yield after each cycle. Nevertheless, PDIs were ≤ 1.6 after each cycle. Ruthenium contaminations of the poly(NBE) materials synthesized were ≤ 75 ppm, which suggested an efficient cleavage of the ruthenium from the growing polymer chain. We therefore attributed the decrease in activity over the cycles to catalyst deactivation. Notably, however, apparently none of the decomposition products ended up in the non-polar phase but remained in the IL phase. This suggested that the ionic ligand adhered to ruthenium also in the decomposition products.

For complexes **3 a** and **5 a**, recycling was possible over several cycles. Catalyst **3 a** was active for 7 cycles, with the 5th cycle carried out 12 h after the 4th. **3 a** proved stable and active for

Table 6. Recycling of **3b**, **3a**, and **5a** in the polymerization of NBE under biphasic conditions.^[a]

Catalyst	Cycle	Yield [%]	M_n (exp.) [g mol ⁻¹]	PDI	cis/trans	Ru contamination [ppm]
3b	1	84	6000	1.4	50:50	75
	2	19	10000	1.6	49:51	66
	3	5	6000	1.6	49:51	35
3a	1	87	7000	4.0	55:45	13
	2	65	68000	2.6	55:45	25
	3	50	345000	2.1	53:47	21
	4	56	25000	3.2	57:43	14
	5	65 ^[b]	69000	4.2	57:43	8
	6	56	116000	4.4	56:44	11
5a	7	50	603000	1.6	57:43	11
	1	92	81000	1.9	59:41	51
	2	100	36000	2.7	58:42	24
	3	92	717000	1.7	57:43	40
	4	100	35000	3.9	60:40	41
	5	37 ^[b]	335000	2.2	58:42	53
	6	9	–	–	58:42	56
	7	–	–	–	–	–

[a] Conditions: $T=40^\circ\text{C}$, $t=2\text{ h}$, catalyst/monomer molar ratio = 1:200; M_n (theor.) = 18800 g mol⁻¹, [catalyst] = 4 mg_{catalyst} per 400 mg_{IL} (8.52 $\mu\text{mol}_{\text{catalyst}}\text{g}_{\text{IL}}^{-1}$), 1.6 mL toluene, [monomer] = 0.425 mol L⁻¹. [b] 12 h between cycle 4 and 5.

more than 36 h under the chosen reaction conditions. Apart from a small drop in yield from the 1st to the 2nd cycle, yields remained constant up to the 7th cycle. PDIs varied between 1.6 and 4.4. Dicationic **3a** also allowed for the most efficient ruthenium removal, leading to poly(NBE) with 8–25 ppm ruthenium, which translated into a ruthenium removal of 99.5–99.8% (Table 6). Yields between 92 and 100% were observed for **5a** within the first 4 cycles. After 12 h, the yields dropped significantly, suggesting a reduced stability of the monocationic catalyst. PDIs were in the range of 1.7–3.9. Notably, low ruthenium contaminations of the polymers between 8 and 85 ppm were determined again, translating into a ruthenium removal of 98–99.8%.

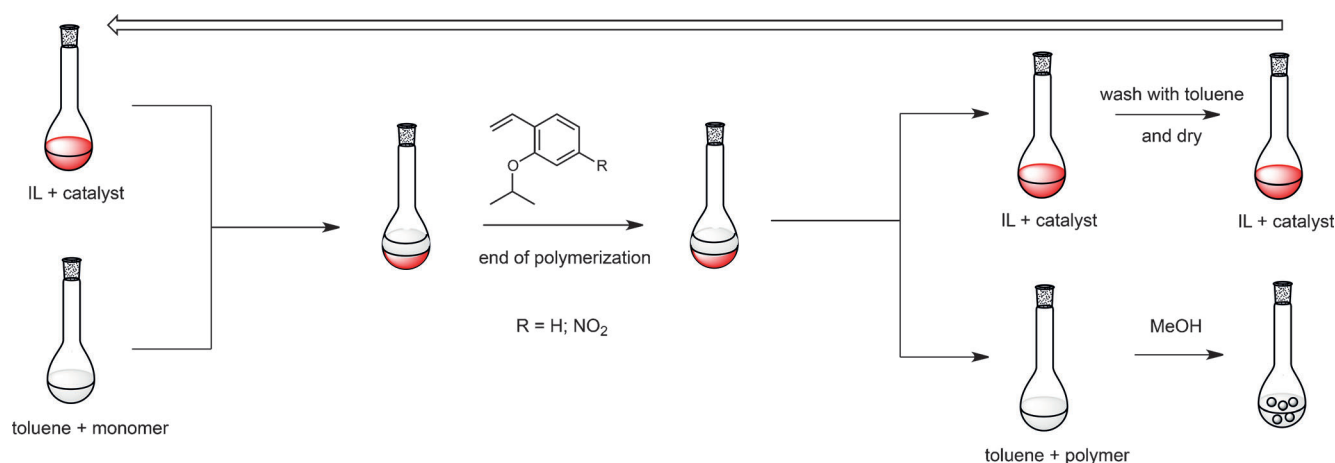
Conclusions

A novel nitro-substituted ionic metathesis catalyst $[\text{Ru}((4\text{-CO}_2)(1\text{-CH}_3)\text{Py}^+)_2(\text{IMesH}_2)(=\text{CH-2-(2-PrO)-5-NO}_2\text{C}_6\text{H}_3)][\text{OTf}^-]_2$ (**3b**) was synthesized. Crystal structures from precursors **2b** and **4b** showed that the replacement of one chloride by one triflate resulted in the shortening of all ruthenium ligand bonds including the ruthenium–oxygen bond in the 2-propoxy group. The shortening of the ruthenium–alkylidene bond was attributed to a stronger polarization of this bond, which in turn explained the higher reactivity of the monoionic complex **5a**. Catalysts **3b**, **3a**, and **5a** were active in ROMP reactions under homogenous conditions, providing good yields. ROMP reactions were also performed under biphasic conditions, allowing the preparation of various NBE-based polymers in high yields. The most striking advantage of the ionic catalysts was that they could be used in a biphasic setup to afford polymers with low metal content, typically in the range between 8 and 80 ppm. Furthermore, multiple recycling was possible under biphasic conditions for catalysts **3a** and **5a**. Again, polymers with low ruthenium contamination were obtained after each cycle. Grubbs–Hoveyda-complexes bearing a nitro-substituted alkylidene did not offer any significant advantages over other initiators and, in the reactions described here, were less stable.

Experimental Section

General

Unless noted otherwise, all manipulations were performed in a Labmaster 130 glovebox (MBraun; Garching, Germany) or by standard Schlenk techniques under N₂ atmosphere. CH₂Cl₂, THF, and diethyl ether (J. T. Baker, Netherlands) were dried by using an MBraun SPS-800 solvent purification system with alumina drying columns. Benzene (VWR) was distilled from sodium and benzophenone under argon. Starting materials were purchased from Aldrich, TCI Europe (Belgium), and ABCR (Germany) and used without further purification. 2-(2-propoxy)-5-nitrostyrene,^[29–31] 2-(2-propoxy)styrene,^[33] $[(1\text{-CH}_3)(4\text{-CO}_2\text{K})\text{Py}^+][\text{BF}_4^-]$ ^[22] and the catalysts $[\text{RuCl}_2(\text{IMesH}_2)(=\text{CH-2-(2-PrO)-5-NO}_2\text{C}_6\text{H}_4)]$,^[29–31] $[\text{RuCl}[(4\text{-CO}_2)(1\text{-CH}_3)\text{Py}^+](\text{IMesH}_2)(=\text{CH-2-(2-PrO)-5-NO}_2\text{C}_6\text{H}_4)]$,^[29–31]



Scheme 4. Illustration of the recycling process.

2-[2-(PrO)C₆H₄][OTf]⁻]^[22] and [Ru{(4-CO₂)(1-CH₃)Py⁺)}₂(IMesH₂)(=CH-2-[2-(PrO)C₆H₄][OTf]⁻)]^[22] were prepared as described.

NMR spectra and resonances were recorded on a Bruker Avance III 400 spectrometer in the indicated solvent at 25 °C and listed in [ppm] downfield from tetramethylsilane as an internal standard. IR spectra were measured on a Bruker IFS 28 using ATR technology and KBr pellets. Gel permeation chromatography measurements were performed on a system consisting of a Waters 515 HPLC pump, a Waters 2707 Autosampler, Polypore columns (300 × 7.5 mm, Agilent technologies, Germany), a Waters 2489 UV/Vis Detector, and a Waters 2414 Refractive Index Detector. For calibration, polystyrene standards with 800 < *M_n* < 2 000 000 g mol⁻¹ were used.

Syntheses

[Ru(CF₃SO₃)₂(IMesH₂)(=CH-2-[2-(PrO)5-NO₂C₆H₃])] (**2b**): Under glovebox conditions, CF₃SO₃Ag (44 mg, 0.34 mmol, 2.4 equiv.) was suspended in CH₂Cl₂ (3 mL) and *N,N*-dimethylformamide (0.05 mL). Then a solution of [RuCl₂(IMesH₂)(=CH-2-[2-(PrO)5-NO₂C₆H₃])] (**1b**, 100 mg, 0.14 mmol, 1 equiv.) in CH₂Cl₂ (2 mL) was added slowly. In the absence of light the vigorously stirred reaction mixture was heated to 35 °C for 5 h, whereby AgCl precipitated. The precipitate was filtered off and the solution evaporated to dryness. The solid was redissolved in CH₂Cl₂ (3 mL) and flashed over a short pad of silica gel. Upon solvent removal, **2b** was obtained as a dark green solid. Yield: 89 mg (0.11 mmol, 76 %); ¹H NMR (400.13 MHz, CD₂Cl₂): δ = 1.20 (d, 6H, *J* = 6.0 Hz), 2.24 (s, 6H), 2.41 (s, 6H), 2.47 (s, 3H), 2.58 (s, 3H), 4.27 (s, 4H), 4.87 (sept, 1H, *J* = 6.0 Hz), 7.00 (d, 1H, *J* = 9.2 Hz), 7.25 (s, 4H), 8.05 (d, 1H, *J* = 2.8 Hz), 8.52 (dd, 1H, *J* = 9.2, 2.8 Hz), 18.68 ppm (s, 1H); ¹³C NMR (100.61 MHz, CDCl₃): δ = 3.7, 4.5, 6.1, 7.0, 36.7, 66.2, 99.4, 101.8, 103.7, 105.0, 113.5, 114.4, 116.0, 116.2, 117.2, 121.7, 121.7, 126.0, 126.9, 127.3, 129.2, 131.5, 144.9, 186.2, 316.6 ppm; ¹⁹F NMR (376.50 MHz, CD₂Cl₂): -77.28 ppm; IR (KBr): $\tilde{\nu}$ = 2921, 2865, 1607, 1580, 1485, 1332, 1268, 1227, 1175, 1090, 1023, 975, 907, 858, 827, 744, 631, 575, 514, 441, 419 cm⁻¹; Elemental analysis (%) calcd. for C₃₃H₃₈F₆N₃O₉RuS₂ (899.86): C 44.05, H 4.26, N 4.67; found: C 44.44, H 4.09, N 4.51.

[Ru{(4-CO₂)(1-CH₃)Py⁺)}₂(IMesH₂)(=CH-2-[2-(PrO)5-NO₂C₆H₃][OTf]⁻)] (**3b**): Under glovebox conditions, the ionic ligand [(1-CH₃)(4-CO₂K)Py⁺][BF₄⁻] (26.9 mg, 0.102 mmol) was suspended in CH₂Cl₂ and a solution of [Ru(CF₃SO₃)₂(IMesH₂)(=CH-2-[2-(PrO)5-NO₂C₆H₃])] (**2b**, 40.0 mg, 0.044 mmol) in CH₂Cl₂ was added slowly to the stirred solution. Stirring was continued for 7 h, the reaction mixture was filtered through Celite, and the residual solid dried in vacuo. A red-brown solid was obtained. Yield: 16 mg (31 %); ¹H NMR (400.13 MHz, CD₂Cl₂): δ = 0.88 (d, 6H, *J* = 6.4 Hz), 2.26 (s, 6H), 2.05 (s, 6H), 2.24 (s, 12H), 3.95 (s, 4H), 4.40 (s, 6H), 4.63 (sept, 1H, *J* = 6.0 Hz), 6.76 (s, 4H), 6.79 (s, 1H), 7.93 (d, 4H, 6.4 Hz), 8.29 (m, 2H), 8.72 (d, 1H, *J* = 6.8 Hz), 18.18 ppm (s, 1H); ¹³C NMR (100.61 MHz, [D₆]DMSO): δ = 29.6, 31.6, 32.0, 32.2, 32.9, 33.1, 37.9, 35.2, 36.1, 36.2, 62.3, 65.2, 66.3, 79.4, 86.6, 128.0, 133.6, 136.8, 140.0, 140.2, 141.1, 142.5, 143.3, 143.7, 144.1, 149.9, 150.2, 150.6, 151.6, 151.8, 152.0, 152.4, 153.2, 154.7, 155.3, 160.4, 160.8, 161.2, 167.1, 183.0, 185.3, 218.6, 325.7 ppm; ¹⁹F NMR (376.50 MHz, CD₂Cl₂): -78.95 ppm; IR (KBr): $\tilde{\nu}$ = 3056, 2982, 2890, 1952, 1642, 1606, 1576, 1520, 1481, 1416, 1342, 1265, 1221, 1149, 1090, 1027, 946, 916, 857, 770, 747, 684, 637, 572, 515, 475, 425 cm⁻¹; Elemental analysis (%) calcd. for C₄₇H₅₂F₆N₅O₁₃RuS₂ (1174.13): C 48.08, H 4.46, N 5.96; found: C 48.15, H 4.56, N 5.93.

[RuCl(CF₃SO₃)(IMesH₂)(=CH-2-[2-(PrO)5-NO₂C₆H₃])] (**4b**): Under glovebox conditions, [RuCl₂(IMesH₂)(=CH-2-[2-(PrO)5-NO₂C₆H₄])] (**1b**, 200 mg, 0.30 mmol) was dissolved in THF (10 mL) and a solution of

CF₃SO₃Ag (1 equiv., 76.6 mg, 0.30 mmol) in THF (2 mL) was added slowly to the stirred solution. Stirring was continued for 2 h. A color change from green to dark green and the formation of a precipitate were observed. The precipitate was filtered off and the solution evaporated to dryness. The solid was dissolved in CH₂Cl₂, filtered through Celite, and dried in vacuo. Recrystallization from *n*-hexane provided the pure product as a green solid. Yield: 234 mg (80 %); ¹H NMR (400.13 MHz, CDCl₃): δ = 1.14 (d, 3H, *J* = 8.0 Hz), 1.36 (d, 3H, *J* = 8.0 Hz), 2.21 (s, 3H), 2.34 (s, 3H), 2.40 (d, 6H, *J* = 5.2 Hz), 2.54 (s, 3H), 2.61 (s, 3H), 4.24 (s, 4H), 4.90 (sept, 1H, *J* = 6.4 Hz), 6.91 (d, 1H, *J* = 8.8 Hz), 7.09 (s, 2H), 7.16 (s, 1H), 7.28 (s, 1H), 7.92 (d, 1H, *J* = 2.8 Hz), 8.48 (dd, 1H, *J* = 8.8, 2.8 Hz), 17.53 ppm (s, 1H); ¹³C NMR (100.61 MHz, CDCl₃): δ = 17.1, 17.4, 18.2, 19.4, 19.6, 20.3, 20.5, 50.2, 52.1, 78.2, 112.6, 116.6, 125.3, 129.0, 129.2, 129.4, 129.5, 131.8, 136.1, 137.4, 139.2, 139.7, 140.0, 142.7, 144.7, 156.8, 203.9, 309.6 ppm; ¹⁹F NMR (376.50 MHz, CD₂Cl₂): -77.17 ppm; IR (KBr): $\tilde{\nu}$ = 2920, 2865, 1605, 1570, 1483, 1338, 1325, 1229, 1265, 1197, 1178, 1010, 746, 627, 574, 516, 420 cm⁻¹; Elemental analysis (%) calcd. for C₃₂H₃₈ClF₃N₃O₆RuS (786.24): C 48.88, H 4.87, N 5.34; found: C 49.04, H 4.81, N 5.19.

General method for ROMP

ROMP polymers were prepared as follows: the catalyst (1.0 mg, 0.9 μmol for **3b**, 0.9 μmol mol for **3a**, 1.4 μmol for **5a**) was dissolved in CH₂Cl₂ (0.5 mL) then added to a solution containing the monomer (see Table 5 for details) in CH₂Cl₂ (1.5 mL). The mixture was stirred for 1–2 h at the indicated temperature. Then, ethyl vinyl ether was added and stirring was continued for another 30 min. A major part of the solvent was removed in vacuo, then the polymer was precipitated from methanol.

ROMP under biphasic conditions

The catalyst (4.0 mg, 3.41 μmol for **3b**; 3.54 μmol for **3a**; 5.48 μmol for **5a**) was dissolved in [BDMIM⁺][BF₄⁻] IL at 40 °C. A solution of the monomer (catalyst/monomer molar ratio = 1:200) in toluene (1.6 mL, 0.425 mol L⁻¹) was added. The mixture was stirred for 2 h, then a solution of 2-(2-propoxy)-5-nitrostyrene (for **3b**, 100 equiv.) or of 2-(2-propoxy)styrene (for **3a** and **5a**, 100 equiv.) in toluene (2 mL, 0.169 mol L⁻¹) was added. After 1 h at 40 °C, toluene (2 mL) was added and the solution was stirred for another 5 min. Stirring was stopped and after phase separation had occurred, the polymer-containing phase on the top was removed. The IL phase was then extracted with toluene (5 × 2 mL). After combining the toluene fractions, the solvent was removed in vacuo to yield the polymer.

Recycling

The same polymerization procedure as described above for the ROMP under biphasic conditions was used. After washing, a new portion of monomer solution was added and polymerization was restarted. The procedure was repeated several times as shown in Table 6.

Ruthenium measurements

The Ru content of the polymers was determined by using inductively coupled plasma optical emission spectroscopy (ICP-OES). Samples were prepared by adding aqua regia to samples of the polymer (20.0 mg). The mixture was placed inside high-pressure

Teflon tubes and leaching was performed under microwave conditions (600, 800, and 0 W pulses, respectively, $t=2.83$ h). After cooling to RT, the mixture was filtered and ICP-OES measurements for Ru were taken ($\lambda=240.272$ nm, ion line, background lines at $\lambda_1=240.254$ nm and $\lambda_2=240.295$ nm) by using a Spectro Arcos device (Ametek GmbH; Meerbusch, Germany). Standardization was performed with Ru standards containing 0.1, 0.5, 1.0, 2.5, and 5 ppm Ru.

X-ray measurements and structural determination of 2b and 4b

Data were collected on a Kappa Apex 2 duo diffractometer at -173°C . The structure was solved by using direct methods with refinement by full-matrix least squares on F^2 , with the program system SHELXL 97 in connection with a multiscan absorption correction. All non-hydrogen atoms were refined anisotropically. Supplementary crystallographic data can be obtained free of charge from the Cambridge Crystallographic Centre via www.ccdc.cam.ac.uk/data_request/cif.

Acknowledgements

The authors wish to thank Dipl.-Chem. S. Naumann (University of Stuttgart) for his help with ICP-OES measurements. B.A. is grateful for the financial support provided by the Deutsche Forschungsgemeinschaft (DFG, grant no. BU 2174/8-1). C.P.F. is grateful for the financial support provided by CAPES (Coordenação de Aperfeiçoamento de Pessoal de Nível Superior, process no. 8924-12-0) and to her supervisor Prof. Benedito S. Lima-Neto, Instituto de Química de São Carlos, Universidade de São Paulo.

Keywords: biphasic catalysis • ionic initiators • recycling • romp • ruthenium

- [1] M. R. Buchmeiser, *Chem. Rev.* **2000**, *100*, 1565.
[2] R. H. Grubbs, *Handbook of Metathesis*, Wiley-VCH, Weinheim, Germany, **2003**.
[3] R. H. Grubbs, S. Chang, *Tetrahedron* **1998**, *54*, 4413–4450.
[4] A. H. Hoveyda, R. R. Schrock, *Chem. Eur. J.* **2001**, *7*, 945–950.
[5] S. Kotha, M. K. Dipak, *Tetrahedron* **2012**, *68*, 397–421.
[6] T. M. Trnka, R. H. Grubbs, *Acc. Chem. Res.* **2000**, *34*, 118.
[7] M. R. Buchmeiser, *New J. Chem.* **2004**, *28*, 549–557.
[8] M. R. Buchmeiser, *Catal. Today* **2005**, *105*, 612.
[9] J. H. Cho, B. M. Kim, *Org. Lett.* **2003**, *5*, 531–533.
[10] M. Mayr, B. Mayr, M. R. Buchmeiser in *Studies in Surface Science and Catalysis 143* (Ed.: E. Gaigneaux), Elsevier Science B. V., **2002**.
[11] S. W. Chen, J. H. Kim, K. Y. Ryu, W. W. Lee, J. Hong, *Tetrahedron* **2009**, *65*, 3397–3403.
[12] H. Clavier, K. Grela, A. Kirschning, M. Mauduit, S. P. Nolan, *Angew. Chem.* **2007**, *119*, 6906–6922; *Angew. Chem. Int. Ed.* **2007**, *46*, 6786–6801.
[13] C. Copéret, J.-M. Basset, *Adv. Synth. Catal.* **2007**, *349*, 78–92.
[14] I. Dragutan, V. Dragutan, *Platinum Met. Rev.* **2008**, *52*, 71–82.
[15] A. H. Hoveyda, D. C. Gillingham, J. J. Van Veldhuizen, O. Kataoka, S. B. Garber, J. S. Kingsbury, *Org. Biomol. Chem.* **2004**, *2*, 8–23.
[16] S. C. Schürer, S. Gessler, N. Buschmann, S. Blechert, *Angew. Chem.* **2000**, *112*, 4062–4065.
[17] Q. W. Yao, *Angew. Chem.* **2000**, *112*, 4060–4062; *Angew. Chem. Int. Ed.* **2000**, *39*, 3896–3898.
[18] H. Balcar, D. Bek, J. Sedlacek, J. Dedecek, Z. Bastl, M. Lamac, *J. Mol. Catal. A-Chem.* **2010**, *332*, 19–24.
[19] M. Bru, R. Dehn, J. H. Teles, S. Deuerlein, M. Danz, I. B. Müller, M. Limbach, *Chem. Eur. J.* **2013**, *19*, 11661.
[20] B. van Berlo, K. Houthoofd, B. F. Sels, P. A. Jacobs, *Adv. Synth. Catal.* **2008**, *350*, 1949–1953.
[21] B. Autenrieth, W. Frey, M. R. Buchmeiser, *Chem. Eur. J.* **2012**, *18*, 14069–14078.
[22] B. Autenrieth, F. Willig, D. Pursley, S. Naumann, M. R. Buchmeiser, *ChemCatChem* **2013**, *5*, 3033–3040.
[23] M. Al-Hashimi, C. Hongfa, B. George, H. S. Bazzi, D. E. Bergbreiter, *J. Polym. Sci. Part A* **2012**, *50*, 3954–3959.
[24] D. Bek, H. Balcar, N. Zilkova, A. Zukal, M. Horacek, J. Cejka, *ACS Catal.* **2011**, *1*, 709–718.
[25] K. Breitenkamp, T. Emrick, *J. Polym. Sci. Part A* **2005**, *43*, 5715–5721.
[26] K. Melis, D. De Vos, P. Jacobs, F. Verpoort, *J. Mol. Catal. A-Chem.* **2001**, *169*, 47–56.
[27] S. Csihony, C. Fischmeister, C. Bruneau, I. T. Horvath, P. H. Dixneuf, *New J. Chem.* **2002**, *26*, 1667–1670.
[28] Y. S. Vygodskii, A. S. Shaplov, E. I. Lozinskaya, O. A. Filippov, E. A. Shubina, R. Bandari, M. R. Buchmeiser, *Macromolecules* **2006**, *39*, 7821–7830.
[29] M. Bieniek, A. Michrowska, J. Gulajski, K. Grela, *Organometallics* **2007**, *26*, 1096–1099.
[30] K. Grela, A. Michrowska, *Angew. Chem.* **2002**, *114*, 4210; *Angew. Chem. Int. Ed.* **2002**, *41*, 4038.
[31] A. Michrowska, R. Bujok, S. Harutyunyan, V. Sashuk, G. Dolognos, K. Grela, *J. Am. Chem. Soc.* **2004**, *126*, 9318–9325.
[32] J. O. Krause, O. Nuyken, K. Wurst, M. R. Buchmeiser, *Chem. Eur. J.* **2004**, *10*, 777–784.
[33] S. B. Garber, J. S. Kingsbury, B. L. Gray, A. H. Hoveyda, *J. Am. Chem. Soc.* **2000**, *122*, 8168.
[34] J. O. Krause, O. Nuyken, M. R. Buchmeiser, *Chem. Eur. J.* **2004**, *10*, 2029–2035.
[35] M. R. Buchmeiser, I. Ahmad, V. Gurram, P. S. Kumar, *Macromolecules* **2011**, *44*, 4098–4106.
[36] S. Sutthasupa, F. Sanda, T. Masuda, *Macromol. Chem. Phys.* **2008**, *209*, 930–937.
[37] G. C. Bazan, E. Khosravi, R. R. Schrock, W. J. Feast, V. C. Gibson, W. M. Davis, *J. Am. Chem. Soc.* **1990**, *112*, 8378.
[38] J. Alonso-Villanueva, J. M. Cuevas, J. M. Laza, J. L. Vilas, L. M. Leon, *J. Appl. Polym. Sci.* **2010**, *115*, 2440–2447.
[39] C. W. Bielawski, D. Benitez, T. Morita, R. H. Grubbs, *Macromolecules* **2001**, *34*, 8610–8618.

Received: September 6, 2013

Published online on October 31, 2013